

Evaluation of the Effect of Nano-Sodium Alginate-Bioglass on Cardiac Function of Myocardial Infarction Based on Cardiac Ultrasound

Tao Guan[#], Xiaoshuang Zhu[#], Lihua Tian^{*}, Tingting Shen^{*}

Department of Ultrasound, Xiangyang Central Hospital, Affiliated Hospital of Hubei University of Arts and Science, Xiangyang, 441000, China

[#]These authors contributed equally to this work as co-first author

ARTICLE INFO

Original paper

Article history:

Received: October 12, 2021

Accepted: March 20, 2022

Published: March 31, 2022

Keywords:

Ultrasonic Evaluation, Nano-Sodium Alginate-Bioglass, Myocardial Infarction, Cardiac Function

ABSTRACT

In cardiovascular diseases, myocardial infarction is the most important cause of chronic heart failure. According to reports, more than 70% of patients with chronic heart failure suffer from myocardial infarction. Nano sodium alginate-bioglass has attracted more and more attention in the treatment of myocardial infarction due to its good cell proliferation. In order to understand the effect of nano-sodium alginate-bioglass on myocardial infarction, we added nano-sodium alginate-bioglass in the treatment process. The calcium ions released by the bio-glass during the slurry preparation process partially cross-link the sodium alginate, which helps to restore the heart function of myocardial infarction. Add nano-seaweed Sodium-bioglass can significantly promote the proliferation of heart cells. Through the test of different groups and the results of cell experiments, we have obtained the best recovery effect of myocardial infarction when the bioglass content is about 30%, and the changes in the vitality of heart cells can be seen most clearly.

DOI: <http://dx.doi.org/10.14715/cmb/2022.68.3.9>

Copyright: © 2022 by the C.M.B. Association. All rights reserved.



Introduction

After myocardial infarction, the excessive volume of body fluid in the left ventricle leads to an increase in ventricular wall stress, which leads to the sliding of the cardiomyocyte layer in the infarct area, resulting in the expansion of the infarct area. In addition, under the action of various neurosynthetic fluid factors, cardiomyocytes hypertrophy, mortality, changes in the extracellular matrix and cardiomyocyte composition, and cardiomyocytes hypertrophy and elongation in non-infarct areas (1). Therefore, the evaluation of the shape and function of the heart must be carried out in three-dimensional space. In recent years, with the rapid development of computer technology, dynamic three-dimensional ultrasound (3DE) has been used in the measurement of myocardial weight, the evaluation of the cardiac structure, the measurement of cardiac cavity volume and so on (2).

Ventricular reset rings can be detected by cardiac echo, CT, MRI, left ventricular catheterization, radionuclide myocardial imaging and other methods. Among them, radionuclide myocardial imaging is unique in evaluating left ventricular severity after

myocardial infarction (3). Not only the previous myocardial perfusion imaging but also the parameters of EDV, ESV and EF can be obtained. This method is non-invasive. It can continuously, quantitatively, and qualitatively observe the changes in myocardial perfusion and left ventricular remodeling after myocardial infarction. It can be observed that the absorption function of cardiomyocytes is before the changes in the cardiac structure after myocardial infarction. Evaluate the disease development that can play a role at any time, and provide a convenient, accurate and reliable objective basis for the clinic.

In recent years, nano sodium alginate Bioglass has been widely used in clinical trials of myocardial infarction. Carlsson A.C. believes that highly sensitive cardiac troponin T (HS cTnT) has recently been introduced into clinical practice, increasing sensitivity and reducing specificity (4). He aimed to identify predictors and prevalence of HS cTnT levels above the 99th percentile in a stable population of patients without myocardial infarction (MI) who were treated in the emergency department due to chest pain. He included 11847 patients with chest pain and

*Corresponding author. E-mail: shenrong639962@163.com; dulanmu1857375024@163.com
Cellular and Molecular Biology, 2022, 68(3): 67-76

performed at least one HS cTnT measurement. He used logistic regression to calculate the adjusted odds ratio of the 95% confidence interval for the association between patient characteristics and HS cTnT level > 14 ng / L. He also determined the 50th, 75th, 97.5 and 99th percentile values of HS cTnT levels related to age, gender, estimated glomerular filtration rate (EGFR), and the presence of comorbidity. HS cTnT levels above the 99th percentile are common in patients with chest pain but no myocardial infarction and are associated with gender, age and EGFR. Lang C believes that stem cell-based regenerative therapy for ischemic myocardium is an in-depth research topic. In human phase, I and phase II clinical trials, a variety of cell populations have been proved to be safe and played some positive roles, but there is still a lack of conclusive evidence of effectiveness. In the context of hundreds of preclinical studies evaluating the efficacy of a variety of cell preparations (including pluripotent stem cells) for heart repair, he systematically reassessed the data of mouse models, which initially paved the way for the first clinical trial in this field. He conducted a systematic literature screening to identify publications reporting the results of cardiac stem cell therapy in the treatment of myocardial ischemia in mouse models. Only peer-reviewed and placebo-controlled studies using magnetic resonance imaging (MRI) to assess left ventricular ejection fraction (LVEF) were included. Mice are an effective model to evaluate the efficacy of advanced cell-based therapy in the treatment of the ischemic myocardial injury. Further research is needed to understand the mechanism of stem cell-based cardiac function improvement after ischemia (5). Spadaccio C believes that the previously developed poly L-lactide scaffold releasing granulocyte colony-stimulating factor (PLLA / GCSF) was tested as a ventricular patch in a rabbit model of chronic myocardial infarction (MI). The control group consisted of healthy, chronic myocardial infarction and nonfunctional PLLA stents. PLLA-based electrospun stents were effectively integrated into chronic infarcted myocardium. These findings, combined with the reduction of end-systolic and end-diastolic volumes, indicate the preventive effect of stents on ventricular dilation and the improvement of cardiac performance (6). Monte Carlo C believes that the autopsy diagnosis of early

myocardial infarction is a challenge for forensic pathologists because conventional histology has no specificity. Many authors suggest the use of immunohistochemistry to fill the gap in the histological diagnosis of early myocardial infarction. He aimed to analyze the progress of immunohistochemical detection of early ischemic heart injury. To this end, he reviewed experimental studies on immunohistochemical markers and their expression time. The literature review emphasizes that the markers analyzed are complement components, others are inflammatory mediators, cardiomyocyte proteins, plasma proteins, stress or hypoxia-inducible factors and proteins related to heart failure (7). Schiele f believes that medical quality assessment is an integral part of modern medical care and has become an indispensable tool for health authorities, the public, the media and patients. However, it is difficult to measure the quality of nursing, because it is a multi-factor and multi-level concept, which can not be evaluated only according to the clinical results of patients. Therefore, in this regard, it has become a widely used practice to measure the nursing process through quality indicators (QI). In this context, the European Society of Cardiology (ESC) acute cardiovascular care association (ACCA) reflected on the measurement of nursing quality of AMI and created a set of Qi to formulate plans to improve the nursing quality of AMI management in Europe. Here he provides a list of qualified intermediaries defined by ACCA and explains the methods used the scientific basis and the reasons for choosing each measure (8).

Acute myocardial infarction and heart failure is a disease that has a serious impact on human health. The incidence is very high in European and American countries, and the death from various causes ranks first. In recent years, with the development of the economy and the change in people's living environment, the incidence in China has increased year by year, close to the international average level. In order to treat myocardial infarction, nano sodium alginate Bioglass was applied in the field of myocardial infarction in various ways. To evaluate the improvement of cardiac function before and after ultrasonic transplantation, and provide the basis for the selection of clinical transplantation path for the improvement of cardiac function after stem cell transplantation.

Evaluating the Effect of Nano-Sodium Alginate-Bioglass on Cardiac Function of Myocardial Infarction by Echocardiography Nano Sodium Alginate-Bioglass

The nano-rheological test experiment is very sensitive to the structural changes of the nano-fluid system and is a very effective method to characterize the structure and performance of the nano-fluid system. Rheological experiments under steady-state include static velocity scanning and vertical circulation. Through the steady-state velocity scanning experiment, the relationship between the shear rate of the system and the apparent viscosity and vertical stress difference can be determined, so nanofluids can be obtained (9). Some information and trigger cycles can analyze the corresponding internal structure according to the change in the shear speed. When the Euclidean distance is selected as the vector x_k in group i as the index of dissimilarity with the corresponding cluster center c_i , the objective function can be defined as (10):

$$J = \sum_{i=1}^c J_i = \sum_{i=1}^c \left(\sum_{k: x_k \in G_i} \|x_k - c_i\|^2 \right) \tag{1}$$

The objective function of FCM is as follows (11):

$$J_m(U, P) = \sum_{i=1}^c \sum_{j=1}^n u_{ij}^m d_{ij}^2 \tag{2}$$

The probability of the appearance of the pixel with the gray level i is approximated by its frequency, then the normalized histogram of the image I is (12):

$$H = \{p_0, p_1, \dots, p_{L-1}\}, \sum_{i=0}^{L-1} p_i = 1 \tag{3}$$

According to the calculation method of the mean value of random variables in probability theory, the intra-class gray values of pixels assigned to the background B class and the target O class are respectively (13):

$$\mu_B(t) = \frac{1}{P_B(t)} \sum_{i=0}^t ip_i, \mu_O(t) = \frac{1}{P_O(t)} \sum_{i=t+1}^{L-1} ip_i \tag{4}$$

The average gray level is:

$$\mu = \sum_{i=0}^{L-1} ip_i \tag{5}$$

The gray mean square error of all pixels is (14):

$$\sigma^2 = E[(i - \mu)^2] = \sum_{i=0}^{L-1} p_i (i - \mu)^2 \tag{6}$$

Use the gradient method to find the minimum value of $J_{PCM}(U, P)$ on the parameters u_{ij} and c_i , and get the iterative formula of u_{ij} , c_i (15):

$$c_i = \frac{\sum_{j=1}^n u_{ij}^m x_j}{\sum_{s=1}^n u_{is}^m} \tag{7}$$

$$u_{ij} = \frac{1}{1 + \left[\frac{d_{ij}^2}{\eta_i} \right]^{1/(m-1)}} \tag{8}$$

According to the definition of Tsallis entropy, the two-dimensional Tsallis entropy of the background and target can be defined as follows (16,17):

$$S_q^B(t, s) = \frac{1 - \sum_{i=0}^t \sum_{j=0}^s \left(\frac{p(i, j)}{P_2(t, s)} \right)^q}{q - 1} \tag{9}$$

$$S_q^O(t, s) = \frac{1 - \sum_{i=t+1}^{L-1} \sum_{j=s+1}^{L-1} \left(\frac{p(i, j)}{P_4(t, s)} \right)^q}{q - 1} \tag{10}$$

Experimental Equipment and Reagents

The main instruments used in the experiment are as follows: HJ-multi-head constant temperature heating magnetic stirrer; SKC-211C constant temperature shaker; AL104 precision electronic analytical balance; RF-5301PC type fluorescence spectrophotometer; PHS3CW type pH meter; VC750 ultrasonic cell crusher; WFZ-26A type dual-beam UV-visible spectrophotometer; FTIR-8201 Fourier transform infrared spectrometer, etc. (18).

The main reagents used in the experiment are as follows: sodium alginate; dialysis bag; methyl oleate; formamide, etc. (19).

Preparation of Nano Sodium Alginate-Bioglass

In the experiment, water is the continuous phase and fragrance is the dispersed phase. Due to the action of the emulsifier and external force, the citrus fragrance is evenly dispersed during the continuous phase, forming an underwater oil-type emulsification system. Using the ion exchange reaction of Na^+ on the

G segment of sodium alginate and Ca^{2+} in calcium chloride, aromatic molecules were encapsulated to prepare nano-sodium alginate-bioglass. At the same time, the oil-soluble essence is emulsified under the action of the emulsifier, and then forms small droplets of essential oil under the action of ultrasound, which are evenly dispersed in the continuous phase. Under the action of magnetic stirring, calcium chloride finally exchanges ions with sodium alginate, and the molecular chains are entangled and condensed to form bioglass, and aromatic molecules are encapsulated in it. Heat the calcium chloride aqueous solution to 45°C with a digital display magnet (20,21). The schematic diagram of the formation of nano sodium alginate-bioglass is shown in Figure 1.

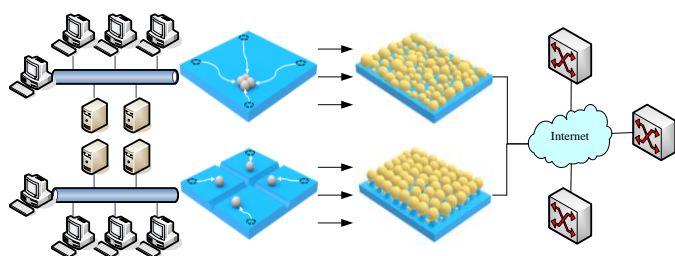


Figure 1. Schematic diagram of the formation of nano-sodium alginate-bioglass

Research Objects

Fifty-one patients with coronary heart disease were selected. All patients underwent coronary angiography. There was at least one main coronary artery with stenosis of more than 70%, of which 5.9% was complete occlusion and 7.8% was sub-total occlusion. The selected medical records are suitable for the reconstruction of coronary circulation associated with infarction, without congenital, hypertensive and valvular heart disease (22). Among 51 patients, 25 patients successfully underwent coronary artery blood circulation reconstruction related to infarction, and 26 patients met the above conditions but failed to accept coronary artery blood circulation reconstruction related to infarction due to various other reasons (23,24). 51 patients were divided into two groups: the myocardial infarction group and the control group.

Echocardiographic Examination

Siemens accuson sequoia 512 and wide color Doppler ultrasonic diagnostic device are used, the

detection frequency is 3.5MHz, and the ultrasonic data are saved on an optical disk for analysis and observation. The patient was in the left decubitus position, breathing steadily, and ECG was displayed at the same time. According to the recommendation of the American echocardiography Association, a standard two-dimensional echocardiogram was performed. The thickness of the ventricular septum and left ventricular posterior wall and diameter of the left ventricle (LVDD, LVD) were measured (25). In 4 information block views and 2 information block views, the simplified symbolic method was used to measure the left ventricular volume (EDV, ESV) and calculate LVEF. The pulse-Doppler sampling volume is set between the heart valve tips of the extended period cap valve, and the detection position and direction are carefully adjusted to make the sound beam parallel to the direction of oral blood flow, so as to obtain the best extended period cap valve in front. Blood flow spectra were collected and the patient's respiratory arrest state was recorded at the end of the expiratory. The measurement indexes include the peak velocity of blood at the initial stage of expansion (E) and the peak velocity of blood at the later stage of expansion (a), and the E / a ratio is calculated (26,27).

Statistical Processing

All measurement data are expressed in the form of average \pm standard deviation. The comparison between the experimental group and the comparison group is carried out by the t-test of independent samples, and the comparison within the group is carried out by the t-test of the corresponding samples. In this experiment, $p < 0.05$ on both sides was considered a significant statistical difference. The statistical analysis involved in this experiment was analyzed using SPSS16.0 version statistical software (28-30).

Effect of Nano Sodium Alginate-Bioglass on Cardiac Function of Myocardial Infarction

The comparison of myocardial myocardial imaging between the myocardial infarction group and the normal control group is shown in Table 1. Compared with the normal control group, the left ventricular end-systolic volume (ESV) and end dilation volume (EDV) of the myocardial infarction group increased, and the left ventricular

excitation rate (LVEF) decreased. Combined with the measurement data, the end-systolic volume and end-dilatation volume of patients with severe post-myocardial infarction of the left ventricle are significantly higher than the normal population, but the motivation rate is opposite, which is lower than the general normal population. Through the test of different groups and the results of cell experiments, we have obtained the best recovery effect of myocardial infarction when the bioglass content is about 30%, and the changes in the vitality of heart cells can be seen most clearly.

Table 1. Comparison of myocardial radionuclide myocardial imaging between the myocardial infarction group and the normal control group

Group	EDV	ESV	LVEF
Control group	95.80±9.62	30.73±8.37	68.06±7.11
Myocardial infarction group	111.65±15.41	51.23±17.71	53.97±10.82

During the 6-month and 12-month follow-up, the patient's psychological echo test results were combined with the patient's psychological echo test results at the time of registration, and the changes in ventricular echo and psychological function of the two groups were observed. Patients who entered the statistical analysis during different follow-up periods were first compared with baseline LVEDD, LVESD, LVEDV, LVESV, and LVEF. The changes in the cardiac ultrasound during the 6-month follow-up period are shown in Table 2. There was no difference between patients with LVEDD, LVESD, LVEDV, LVESV, and LVEF at baseline. After 6 months of treatment, there were no statistically significant changes in LVEDD, LVESD, LVEF, LVEDV and LVESV ($p>0.05$).

Table 2. Changes in cardiac ultrasound during the 6-month follow-up

	Myocardial infarction group		Control group	
	Before treatment	After treatment	Before treatment	After treatment
LVEDD	51.7	49.7	50.3	50.8
LVESD	37.2	36.2	35.2	34.7
LVEDV	132.2	127.7	123.5	125.8
LVESV	65.0	62.0	58.0	56.0
LVEF	50.6	52.9	53.8	56.3

The encapsulation efficiency and drug loading of OA nanoparticles at 10%, 20%, and 40% dosing amounts are shown in Figure 2. Within a certain

range, as the dosage of curcumin increases, the encapsulation efficiency and drug load will increase. However, with the increase in dosage (above 20%), the encapsulation rate shows a downward trend. This is because the carrying capacity of the OA coupler is limited. When the dosage reaches a certain threshold, no more curcumin will be embedded in the hydrophobic microdomains of the nanoparticles. The drug load will increase as the amount of curcumin embedded in it increases, and eventually reach a limit threshold.

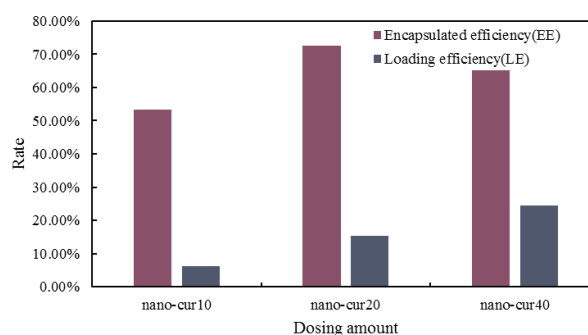


Figure 2. Encapsulation efficiency and drug loading of OA nanoparticles at 10%, 20%, and 40% dosing amount

The killing effect of OA nanoparticles with different concentrations and sizes on MCF-7 cells is shown in Figure 3. As the concentration of nanoparticles increases and the particle size increases, the toxicity increases. But compared with the control group, there is no significant difference. Blank nanoparticles are not enough to cause a strong killing effect on MCF-7 cells, which shows that OA conjugate blank nanoparticles do not have obvious MCF-7 cytotoxicity and are an excellent nano-level drug carrier. Take the rice grain sample as an example, the cell viability is 38.6%, which shows that the killing effect on the cells is obvious.

The release curve of doxorubicin in the drug-loaded micelle AP55 in different concentrations of NaCl solution is shown in Figure 4. When the concentration of NaCl increased from 0 to 0.9%, the drug release rate gradually increased. This is because the salt ions will penetrate and diffuse into the interior of the nanoparticles, thereby shielding the charge on the polyelectrolyte, resulting in the unstable structure of the composite, so some channels will be created, thereby accelerating the drug release rate. From the above results, the sensitivity of this polyelectrolyte

composite micelle to pH and salt provides a unique opportunity to regulate and trigger the release of the loaded drug. This kind of nanoparticle is used as a drug carrier for controlled release by salt concentration.

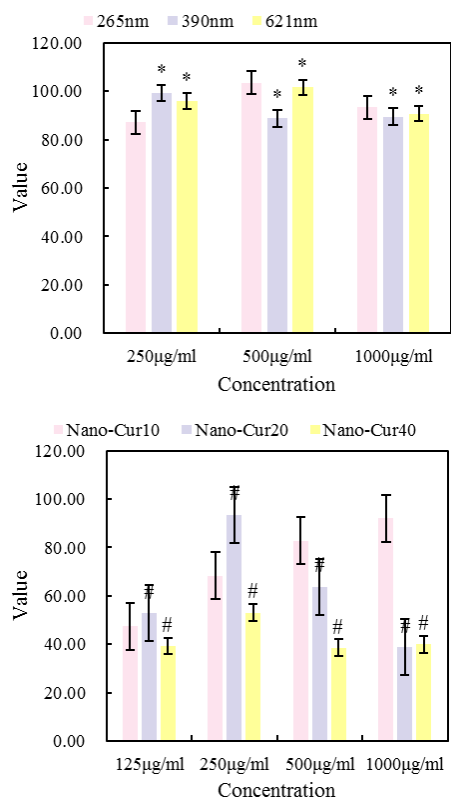


Figure 3. The killing effect of OA nanoparticles with different concentrations and sizes on MCF-7 cells. (* meant that compared with 265nm, the difference was significant, $P<0.05$; # meant that compared with Nano-Cur the difference was significant, $P<0.05$.)

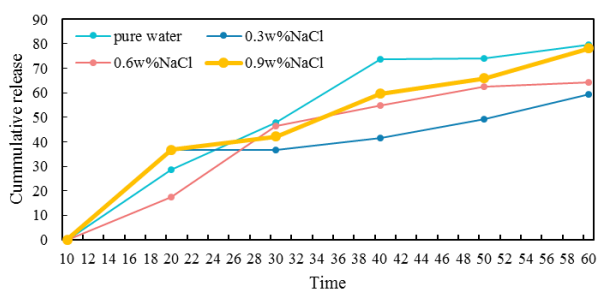


Figure 4. The release curve of doxorubicin in drug-loaded micelle AP55 in different concentrations of NaCl solution

The molecular weights of sodium alginate and nano sodium alginate-bioglass are shown in Table 3. The molecular weight distribution of the nano sodium alginate-bioglass obtained after the reaction of octylamine and sodium alginate broadens

significantly. This may be because the molecular chain of sodium alginate reacts with octylamine. Some molecules bind more octylamine, while some molecules bind. Due to the small number. After the reaction, the molecular weight of the nano sodium alginate-bioglass is slightly smaller than the molecular weight of the sodium alginate before the reaction. This may be caused by a small amount of decomposition of the sodium alginate during the reaction, but the peak molecular weight M_p increased significantly. It also proves that the molecular weight distribution of nano-sodium alginate-bioglass has broadened.

Table 3. The molecular weights of sodium alginate and nano sodium alginate-bioglass

Polymer	Mn	Mw	MP	Mz	Mz+1
Sodium Alginate	302674.7	424152.4	418891	542894.1	651139.7
Nano sodium alginate-bioglass	259525.8	365667.1	531607.7	467405.1	548387.3

The comparison of the ultrasound measurements in the control group during the four follow-ups is shown in Table 4. LVEF is tracked at the time of registration (M0), 6 months after registration (M6), 18 months after registration (M18), and 36 months after registration (M36), M36, M18, M6, and M0. The difference is statistically significant ($p<0.05$). There is no statistically significant difference between M18 and M6 and M0 ($p>0.05$). There is no statistically significant difference between M6 and M0 ($p>0.05$). In the tracking of M36, RVEDV, RVESV, and RVEF were not significantly different from M18, M6 and M0 ($p>0.05$). There is no statistically significant difference between M18, M6, and M0 ($p>0.05$). There is no statistically significant difference between M6 and M0 ($p>0.05$).

Table 4. Comparison of ultrasound measurements in the control group during the four follow-ups

	M0	M6	M18	M36
LVEF	0.32±0.01	0.32±0.01	0.32±0.01	0.31±0.01
RVEDV	108.94±18.84	109.71±17.10	112.44±14.96	113.75±13.70
RVESV	60.45±10.79	60.99±9.88	62.59±8.43	64.07±8.41
RVSV	48.85±9.64	48.09±8.39	48.76±7.12	49.78±6.38
RVEF	0.44±0.031	0.43±0.02	0.43±0.01	0.43±0.02

The comparison of the measured values of the infarcted segment, the adjacent segment and the distal infarcted segment is shown in Figure 5. Compared

with the control group, the rEDV and rESV of the infarcted segment and the infarcted segment increased, and the rEF decreased, the difference was statistically significant ($p < 0.05$), and the rEDV and rESV of the distal infarcted segment increased, and the difference was statistically significant. Academic significance ($p < 0.05$), rEF decreased, and the difference was not statistically significant ($p > 0.05$).

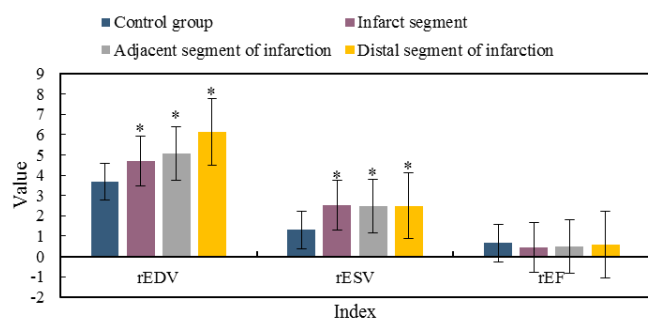


Figure 5. Comparison of measured values of infarcted segment, adjacent segment and distal infarcted segment (* meant that compared with the control group, the difference was significant, $P < 0.05$.)

A two-dimensional echocardiogram was used to evaluate acute myocardial infarction. It was found that the enlargement of the left ventricle included the enlargement of the obstructive area and the enlargement of the whole ventricle. Infarct enlargement within 72 hours after acute myocardial infarction is the main cause of ventricular enlargement in the early stage after myocardial infarction. Within two weeks after infarction, the extension of the ventricular wall without infarction is an important part of the left ventricular redesign. The results of this experiment showed that the volume of the left ventricle at the end of systole and expansion after coronary circulation reconstruction associated with infarction was significantly lower than before. The regional systolic function of the left ventricle 3 months after infarction-related coronary circulation reconstruction was significantly improved compared with that before the operation, which was reflected in the improvement of segmental motion of the ventricular wall. With the improvement of myocardial blood supply, the overall systolic function of the left ventricle is also improved. This is reflected in the significant increase in driving rate and the significant decrease in WMAS. The flow index EI / AI reflecting the left ventricular dilation function of the treatment

group was significantly higher than that of the control group within 3 months after the operation, indicating that infarction-related coronary revascularization can protect or improve the long-term left ventricular dilation function.

Recently, quantitative tissue velocity imaging and distorted velocity imaging based on tissue Doppler can accurately evaluate the function of infarcted myocardium, but they all depend on the angle. Because the vertex is in the front field, it reflects the most realistic result. In the case of the acoustic beam, even the most basic angle requirement of less than 30° is difficult to guarantee. Therefore, these methods are difficult to ensure good accuracy in quantitative analysis of gender psychological function of vertices. RT-3DE is a new technique for measuring cardiac function. It can correctly describe the contour of the left ventricle and analyze the cardiac function of each segment from a three-dimensional point of view. Especially, the quantitative evaluation of the apical part can be performed. Without the limitation of sampling angle, it can more accurately reflect the cardiac function of each segment of the left ventricle. As the main tool to reflect the dynamics of cardiac blood circulation, Doppler cardiac echo examination is widely used in the evaluation of cardiac function. It provides important information for the diagnosis, treatment selection, treatment effect and prognosis of various heart diseases. Continuous observation of the dynamic changes of the endocardial surface can evaluate the changes in left ventricular volume and morphology. Its correctness is confirmed by left ventricular angiography, radionuclide angiography and analysis. The ultrasonic examination will not damage the human body.

The echocardiogram is used to evaluate the effects of various risk factors on psychological function, various treatment methods and diseases of patients with myocardial infarction. Therefore, we can further understand the changes in the left ventricular redesign and cardiac function in patients with coronary heart disease. The effects of left ventricular reduction and cardiac function on the myocardium clarify the effects of various factors on patients with infarction. As a result, in order to prevent severe left ventricular arrhythmia and left ventricular arrhythmia after stroke, we should actively prevent and strictly control hypertension and diabetes, and advocate the treatment

of angiogenesis after myocardial infarction to reduce infarct size and to better understand the methods of improving ventricular heavy and heart.

Sodium alginate is a natural cationic polysaccharide with excellent biocompatibility. It has a wide application prospect in the field of biomedical applications. The characteristics of electronic spinning fiber membrane are small fiber diameter and large specific surface area. If the sodium alginate fiber membrane in the form of electrospinning can be obtained, the application scope of biomedicine can be expanded. The electrospinning seaweed fiber pad not only has a large surface area, but also has the following advantages: porosity, high fiber diameter, lightweight, uniform morphology, high moisture absorption, specific antibacterial properties, flame Retardancy and metal ion adsorption, excellent decomposition, and biocompatibility.

After myocardial infarction, the myocardial contractility in the infarcted area will decrease or even lose. The ventricular wall in the infarct area becomes dilated under the action of ventricular pressure, resulting in the deformation of the cardiac cavity. After the normal myocardial injury, it will activate and produce various neuroendocrine factors, promote cardiomyocyte pathological hypertrophy, cardiomyocyte death, excessive fibrosis or cardiomyocyte extracellular matrix decomposition, and myocardial reset. Next, it causes changes in the overall morphology of the ventricle, that is, ventricular contraction, expansion, late volume increase, and cardiac function injury. At the same time, the deteriorated heart mechanism can activate the neuroendocrine system to produce and form neuroendocrine factors.

Conclusions

This paper compares the local cardiac function of patients with myocardial infarction and healthy people. It is found that the changes in the cardiac systolic function of each part after myocardial infarction have a great impact on the overall cardiac function. Compared with previous myocardial infarctions and other new myocardial infarctions, ultrasonic evaluation technology after myocardial infarction can more accurately evaluate the local cardiac function of the myocardium, especially the evaluation of apical regional cardiac function.

Therefore, the use of ultrasonic evaluation technology can correctly determine the left ventricular segmentation function, help the clinical decision of the treatment plan of myocardial infarction, and play an important role in observing the cure effect and judging the prognosis. At the same time, the experiment shows that the application of nano sodium alginate Bioglass in the clinical treatment of myocardial infarction has a good effect on restoring heart vitality. After myocardial infarction, the local cardiac function of the infarcted myocardium and infarcted myocardium decreases, and the local cardiac function of the distal myocardium is compensated, which plays an important role in maintaining the whole cardiac function after myocardial infarction. Real-time three-dimensional echocardiography can more accurately evaluate the local cardiac function after myocardial infarction, which is conducive to the evaluation of apical myocardial function.

Acknowledgments

Not applicable.

Conflict interest

The authors declare that they have no conflict of interest.

References

1. Chapman AR, Shah ASV, Lee KK, Anand A, Francis O, Adamson P, McAllister DA, Strachan FE, Newby DE, Mills NL. Long-term outcomes in patients with type 2 myocardial infarction and myocardial injury. *Circulation* 2018; 137(12): 1236-1245.
2. Prsbrey M, Raeymaekers B. Ultrasound noncontact particle manipulation of three-dimensional dynamic user-specified patterns of particles in air. *Physical Review Applied* 2018; 10(3): 034066.
3. Hess A, Nekolla SG, Meier M, Bengel FM, Thackeray JT. Accuracy of cardiac functional parameters measured from gated radionuclide myocardial perfusion imaging in mice. *J Nucl Cardiol* 2020; 27(4): 1317-1327.
4. Carlsson AC, Bandstein N, Roos A, Hammarsten O, Holzmann MJ. High-sensitivity cardiac troponin T levels in the emergency department in patients with chest pain but no myocardial infarction. *Int J Cardiol* 2017; 228(13):253-259.
5. Lang CI, Wolfien M, Langenbach A, Müller P, Wolkenhauer O, Yavari A, Ince H, Steinhoff G,

- Krause BJ, David R, Glass Ä. Cardiac Cell Therapies for the Treatment of Acute Myocardial Infarction: A Meta-Analysis from Mouse Studies. *Cell Physiol Biochem* 2017; 42(1):254-268.
6. Spadaccio C, Nappi F, De Marco F, Sedati P, Taffon C, Nenna A, Crescenzi A, Chello M, Trombetta M, Gambardella I, Rainer A. Implantation of a poly-L-lactide GCSF-functionalized scaffold in a model of chronic myocardial infarction. *J Cardiovasc Transl Res* 2017; 10(1):1-19.
 7. Mondello C, Cardia L, Ventura-Spagnolo E. Immunohistochemical detection of early myocardial infarction: a systematic review. *Int J Legal Med* 2017; 131(2):1-11.
 8. Schiele F, Gale CP, Bonnefoy E, Capuano F, Claeys MJ, Danchin N, Fox KA, Huber K, Iakobishvili Z, Lettino M, Quinn T, Rubini Gimenez M, Bøtker HE, Swahn E, Timmis A, Tubaro M, Vrints C, Walker D, Zahger D, Zeymer U, Bueno H. Quality indicators for acute myocardial infarction: A position paper of the Acute Cardiovascular Care Association. *Eur Heart J Acute Cardiovasc Care* 2017; 6(1):34-59.
 9. Belle L, Cayla G, Cottin Y, Coste P, Khalife K, Labèque JN, Farah B, Perret T, Goldstein P, Gueugniaud PY, Braun F, Gauthier J, Gilard M, Le Heuzey JY, Naccache N, Drouet E, Bataille V, Ferrières J, Puymirat E, Schiele F, Simon T, Danchin N. French Registry on Acute ST-elevation and nonST-elevation Myocardial Infarction 2015 (FAST-MI 2015). Design and baseline data. *Arch Cardiovasc Dis* 2017; 110(6-7):366-378.
 10. Waterford SD, Di Eusanio M, Ehrlich MP, Reece TB, Desai ND, Sundt TM, Myrmet T, Gleason TG, Forteza A, de Vincentiis C, DiScipio AW, Montgomery DG, Eagle KA, Isselbacher EM, Muehle A, Shah A, Chou D, Nienaber CA, Khoynezhad A. Postoperative myocardial infarction in acute type A aortic dissection: A report from the International Registry of Acute Aortic Dissection. *J Thorac Cardiovasc Surg* 2017; 153(3):521-527.
 11. Kukreja N, Onuma Y, Garcia-Garcia H, Daemen J, van Domburg R, Serruys PW. Primary percutaneous coronary intervention for acute myocardial infarction: long-term outcome after bare metal and drug-eluting stent implantation. *Circ Cardiovasc Interv* 2017; 10(3):e21-e22.
 12. Kodama N, Nakamura T, Yanishi K, Nakanishi N, Zen K, Yamano T, Shiraishi H, Shirayama T, Shiraishi J, Sawada T, Kohno Y, Kitamura M, Furukawa K, Matoba S. Impact of Door-to-Balloon Time in Patients With ST-Elevation Myocardial Infarction Who Arrived by Self-Transport — Acute Myocardial Infarction-Kyoto Multi-Center Risk Study Group. *Circ J* 2017; 81(11):1693-1698.
 13. Hofmann R, James SK, Jernberg T, Lindahl B, Erlinge D, Witt N, Arefalk G, Frick M, Alfredsson J, Nilsson L, Ravn-Fischer A, Omerovic E, Kellerth T, Sparv D, Ekelund U, Linder R, Ekström M, Laueremann J, Haaga U, Pernow J, Östlund O, Herlitz J, Svensson L; DETO2X–SWEDEHEART Investigators. Oxygen Therapy in Suspected Acute Myocardial Infarction. *N Engl J Med* 2017;377(13):1240-1249.
 14. Dondo TB, Hall M, West RM, Jernberg T, Lindahl B, Bueno H, Danchin N, Deanfield JE, Hemingway H, Fox KAA, Timmis AD, Gale CP. β -Blockers and Mortality After Acute Myocardial Infarction in Patients Without Heart Failure or Ventricular Dysfunction. *J Am Coll Cardiol* 2017;69(22):2710-2720.
 15. Chapman AR, Anand A, Boeddinghaus J, Ferry AV, Sandeman D, Adamson PD, Andrews J, Tan S, Cheng SF, D'Souza M, Orme K, Strachan FE, Nestelberger T, Twerenbold R, Badertscher P, Reichlin T, Gray A, Shah ASV, Mueller C, Newby DE, Mills NL. Comparison of the Efficacy and Safety of Early Rule-Out Pathways for Acute Myocardial Infarction. *Circulation* 2017;135(17):1586-1596.
 16. Pasupathy S, Tavella R, Beltrame J F. Myocardial Infarction With Nonobstructive Coronary Arteries (MINOCA): The Past, Present, and Future Management. *Circulation* 2017; 135(16):1490-1493.
 17. Minamino T, Toba K, Higo S, Nakatani D, Hikoso S, Umegaki M, Yamamoto K, Sawa Y, Aizawa Y, Komuro I; EPO-AMI-II study investigators. Design and rationale of low-dose erythropoietin in patients with ST-segment elevation myocardial infarction (EPO-AMI-II study): a randomized controlled clinical trial. *Cardiovasc Drugs Ther* 2012;26(5):409-16.
 18. Ahmed S M, Abdelrahman S A, Salama A E. Efficacy of gold nanoparticles against isoproterenol induced acute myocardial infarction in adult male albino rats. *Ultrastructural Pathology* 2017; 41(2):168-185.
 19. Keskin K, Sezai Yıldız S, Çetinkal G, Aksan G, Kilci H, Çetin Ş, Sığrırcı S, Kılıçkesmez K. The Value of CHA2DS2VASC Score in Predicting All-Cause Mortality in Patients with ST-Segment Elevation Myocardial Infarction Who Have Undergone Primary Percutaneous Coronary

- Intervention. *Acta Cardiol Sin* 2017;33(6):598-604.
20. Vandergriff A, Huang K, Shen D, Hu S, Hensley MT, Caranasos TG, Qian L, Cheng K. Targeting regenerative exosomes to myocardial infarction using cardiac homing peptide. *Theranostics* 2018;8(7):1869-1878.
 21. Monrad M, Ersbøll AK, Sørensen M, Baastrup R, Hansen B, Gammelmark A, Tjønneland A, Overvad K, Raaschou-Nielsen O. Low-level arsenic in drinking water and risk of incident myocardial infarction: A cohort study. *Environ Res* 2017;154:318-324.
 22. Motovska Z, Hlinomaz O, Kala P, Hromadka M, Knot J, Varvarovsky I, Dusek J, Jarkovsky J, Miklik R, Rokyta R, Tousek F, Kramarikova P, Svoboda M, Majtan B, Simek S, Branny M, Mrozek J, Cervinka P, Ostransky J, Widimsky P; PRAGUE-18 Study Group. 1-Year Outcomes of Patients Undergoing Primary Angioplasty for Myocardial Infarction Treated With Prasugrel Versus Ticagrelor. *J Am Coll Cardiol* 2018;71(4):371-381.
 23. Weichenthal S, Kulka R, Lavigne E, van Rijswijk D, Brauer M, Villeneuve PJ, Stieb D, Joseph L, Burnett RT. Biomass Burning as a Source of Ambient Fine Particulate Air Pollution and Acute Myocardial Infarction. *Epidemiology* 2017; 28(3):329-337.
 24. Dziewierz A, Brener S, Siudak Z, et al. The Interpretation of Genocidal Intent under the Genocide Convention and the Jurisprudence of International Courts. *American Journal of Cardiology* 2018; 78(5):423-441.
 25. Lichtman JH, Leifheit EC, Safdar B, Bao H, Krumholz HM, Lorenze NP, Daneshvar M, Spertus JA, D'Onofrio G. Sex Differences in the Presentation and Perception of Symptoms Among Young Patients With Myocardial Infarction: Evidence from the VIRGO Study (Variation in Recovery: Role of Gender on Outcomes of Young AMI Patients). *Circulation* 2018;137(8):781-790.
 26. Thackeray JT, Hupe HC, Wang Y, Bankstahl JP, Berding G, Ross TL, Bauersachs J, Wollert KC, Bengel FM. Myocardial Inflammation Predicts Remodeling and Neuroinflammation After Myocardial Infarction. *J Am Coll Cardiol* 2018;71(3):263-275.
 27. Wallert J, Lissåker C, Madison G, Held C, Olsson E. Young adulthood cognitive ability predicts statin adherence in middle-aged men after first myocardial infarction: A Swedish National Registry study. *Eur J Prev Cardiol* 2017;24(6):639-646.
 28. Qin C, Gu J, Liu R, Xu F, Qian H, He Q, Meng W. Release of mitochondrial DNA correlates with peak inflammatory cytokines in patients with acute myocardial infarction. *Anatol J Cardiol* 2017; 17(3):224-228.
 29. Alavi, M., Rai, M., Martinez, F., Kahrizi, D., Khan, H., Rose Alencar de Menezes, I., Douglas Melo Coutinho, H., Costa, J. The efficiency of metal, metal oxide, and metalloids nanoparticles against cancer cells and bacterial pathogens: different mechanisms of action. *Cell Mol Biomed Reports*, 2022; 2(1): 10-21. doi: 10.55705/cmbr.2022.147090.1023.
 30. Lee CH, Cheng CL, Kao Yang YH, Chao TH, Chen JY, Li YH. Cardiovascular and Bleeding Risks in Acute Myocardial Infarction Newly Treated With Ticagrelor vs. Clopidogrel in Taiwan. *Circ J* 2018;82(3):747-756.